

# Photoelectric Absorption in the Stellar Wind of the Binary System 4U 1538–52/QV Nor

J. J. Rodes, J. M. Torrejón, and G. Bernabéu

**Abstract** We have used the Rossi X-ray Timing Explorer (RXTE) observatory to analyze the persistent X-ray source 4U 1538–52/QV Nor. The RXTE satellite observed close to one complete binary orbit on January 1997 and 2001 of this X-ray binary system. We have obtained orbital phase resolved spectra to investigate changes in the absorption column density with orbital phase. The variation of the column density over the binary orbit is caused by the movement of the X-ray source through the stellar wind of the companion star. A simple model of absorption in a stellar wind from the companion star described the orbital phase dependence reasonably. From our analysis, we have inferred a wind mass-loss rate from the companion star of  $(1.3 - 2.5) \times 10^{-6} M_{\odot}/\text{yr}$ . Such rate is in agreement with those obtained by the Ginga observations of this X-ray binary pulsar.

## 1 Introduction

Interacting X-ray binary systems, especially supergiant X-ray binaries (SXBs), provide an interesting astrophysical laboratory to test models of the stellar wind of OB stars. SXBs contain either an accreting neutron star or a black hole orbiting within a few stellar radii of the supergiant companion star. The optical counterpart eject much of its mass in the form of a stellar wind and some of this material will be captured gravitationally by the compact object. This is particularly relevant for SXBs systems in a close orbit. Fig. 1 shows a general situation of a compact star accreting from the stellar wind of an early-type companion.

---

J. J. Rodes

Universitat d'Alacant, Apartat de correus 99, E03080 Alacant, Spain e-mail: rodes@dfists.ua.es

J. M. Torrejón

Universitat d'Alacant, e-mail: jmt@dfists.ua.es

G. Bernabéu

Universitat d'Alacant, e-mail: bernabeu@ua.es

Photoelectric absorption estimations through an orbital period provide useful information to test models of the stellar wind of OB stars. The X-ray source is viewed through the stellar wind and is affected by photoelectric absorption in the X-ray spectrum depending on the orbital phases. The absorption increases around the times of eclipse ingress and egress as the compact object passes behind the dense innermost regions of the wind. The accretion process that takes place in SXBs with X-ray luminosities around  $10^{36}$  erg/s is the gravitational capture of a fraction of the stellar wind by the compact object.

The Castor, Abbott and Klein [2] radiatively driven wind theory predicts mass loss rates and terminal velocities for the winds from O stars, early B stars and B supergiants. Steady state theories predict velocity functions in the supersonic regimes of early star winds and mass loss rates that are in general agreement with observations of ultraviolet P Cygni line profiles. One of the SXB systems is the 3.73 days eclipsing system 4U 1538–52 where the optical companion is the B0 I star QV Nor at a distance of  $\sim 5.5$  kpc. The pulse phase averaged X-ray spectrum of this source has been well described by the absorbed Negative Power laws EXponential

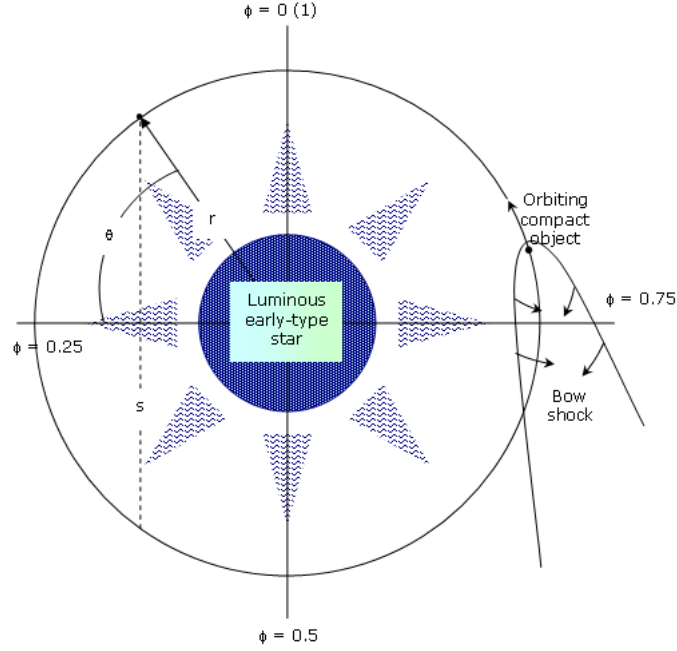


**Fig. 1** In a typical accretion from the stellar wind, the compact object orbits its optical companion in a height above the surface of the optical star of less than one stellar radius, so deeply embedded in the stellar wind of its optical companion. The compact object then accretes from the dense stellar wind and causes the formation of an accretion wake by focusing a significant fraction of the stellar wind. We have assumed a circular orbit whose parameters  $r$ ,  $s$  and  $\theta$  are shown. The orbital phase  $0(1)$  indicates the eclipse

component (NPEX) modified by a fluorescence emission iron line at 6.4 keV and the fundamental Cyclotron Resonant Scattering Feature (CRSF) at 20 keV [12]. In this work we present the variation of the column density against the orbital phase, using two RXTE observations that covers nearly an orbital period each of 4U 1538–52/QV Nor made in 1997 January and 2001 January, respectively. Then we have estimated the mass-loss rate from the accretion of the stellar wind which is in agreement with the results derived from Ginga observations [3].

## 2 Observations and data analysis

RXTE observed the source in 1997 and again in 2001, covering nearly a complete orbital period. The first observation was made on January 01/05 (JD 2,450,449.94 to JD 2,450,453.69) and the second one on January 15/19 (JD 2,451,924.60 to JD 2,451,928.60). We used the best fit orbital ephemeris from [8] to estimate the orbital phase for each observation.

In our analysis we used data from both RXTE pointing instruments, the Proportional Counter Array (PCA) and the High Energy X-ray Timing Experiment (HEXTE). Spectral extractions and background subtractions for both the PCA and HEXTE were performed using the FTOOLS package and spectral models were applied using XSPEC. Both of these software packages were provided by NASA HEASARC.

The PCA consists of five co-aligned Xenon proportional counter units with a total effective area of  $\sim 6000 \text{ cm}^2$  and a nominal energy range from 2 keV to over 60 keV [6]. However, due to response problems above  $\sim 20 \text{ keV}$  and the Xenon-K edge around 30 keV, we restricted the use of the PCA to the energy range from 3 keV to 20 keV [7].

The HEXTE consists of two clusters of four NaI(Tl)/CsI(Na) Phoswich scintillation detectors with a total net detector area of  $1600 \text{ cm}^2$ . These detectors are sensitive from 15 keV to 250 keV [13]. However, response matrix, instrument background and source count rate, limit the energy range from 17 to 100 keV. Background subtraction in HEXTE is done by source-background swapping of the two clusters every 32 s throughout the observation. In order to improve the statistical significance of the data, we added the data of both HEXTE clusters and created an appropriate response matrix by using a 1:0.75 weighting to account for the loss of a detector in the second cluster. We also binned several channels together of the HEXTE data at higher energies and chose the binning as a compromise between increased statistical significance while retaining a reasonable energy resolution.

### 3 Pulse phase averaged spectra analysis and results

The typical continuum spectra of accreting binary pulsars can be described with a power law times exponential cutoff model. We have used the model consists of Negative and Positive power laws with a common EXponential cutoff factor (NPEX [10], [9]). This X-ray continuum approximates a photon number spectrum for an unsaturated thermal comptonization in a plasma temperature  $T$  [9]. We have obtained an acceptable fit with  $\chi^2_{\nu} \leq 1$  for all of the X-ray spectra [11].

The variation of the column density with orbital phase is caused by the movement of the neutron star through the stellar wind of the supergiant companion star. The wind from an early-type star is often modeled as a steady state, spherically symmetric flow where the radial wind velocity takes the form:

$$v_w(r) = v_{\infty} \left(1 - \frac{R_c}{r}\right)^{\alpha}, \quad (1)$$

where  $v_{\infty}$  is the terminal velocity of the wind,  $R_c$  is the radius of the companion star,  $r$  is the distance from the centre of the companion star and  $\alpha$  is the velocity gradient (often in the range 0.7–1.2 for early type stars). Conservation of mass requires:

$$\rho_w = \frac{\dot{M}_c}{4 \pi r^2 v_w}, \quad (2)$$

where  $\dot{M}_c$  is the mass loss rate from the primary and  $\rho_w$  is the wind density. Combining equations 1 and 2 and integrating the wind density along the line of sight to the X-ray source, it will be possible to find a model which describes the variation in  $N_H$  with orbital phase properly. Defining  $s$  as the distance through the stellar wind along the line from the compact object toward the observer (see Fig. 1), we have:

$$N_H = \int_0^s n_H ds \sim n_H s = n_H 2 r \sin \theta. \quad (3)$$

The angle  $\theta$  is related to the orbital phase and equation 3 can be rewritten as:

$$N_H = \frac{\dot{M}_c}{4 \pi r^2 v_{\infty} \left(1 - \frac{R_c}{r}\right)^{\alpha}} 2 r \sin \left(\frac{\pi}{2} - 2 \pi \phi\right). \quad (4)$$

The value of  $N_H$  as a function of orbital phase derived from fitting to the 3–100 keV spectra and the model defined by equation 4 are plotted in Fig. 2.

In order to estimate the mass loss rate from:

$$SN = \frac{\dot{M}_c}{2 \pi r v_{\infty} \left(1 - \frac{R_c}{r}\right)^{\alpha}}, \quad (5)$$

the escape velocity has been estimated as  $690 \pm 50$  km/s [3] according to the relation:

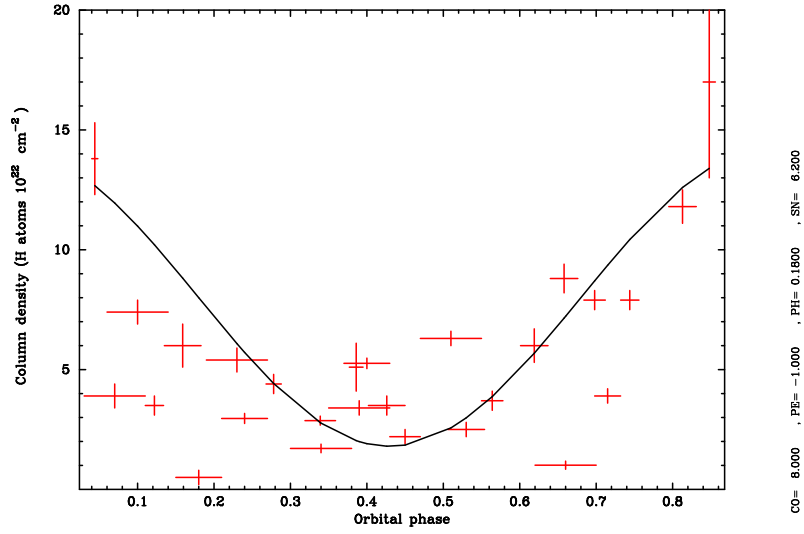


**Fig. 2** Column density ( $N_H$ ) as a function of orbital phase. The values derived from the spectral fits to the RXTE spectra are plotted. The solid line shows the function  $N_H = CO + SN \sin\left(\frac{2\pi(X-PH)}{PE}\right)$ , which is fitted to our data. The bars indicate the uncertainties at 90% confidence level

$$v_{esc} = \sqrt{\frac{2GM(1-\Gamma)}{R}}, \quad (6)$$

where  $\Gamma$  is the ratio of the optical luminosity to the Eddington luminosity.

Next, we took the correlation between  $v_\infty$  and  $v_{esc}$  [1] into account and estimated the range of the terminal velocities for stars of luminosity class I, 1400–2800 km/s. Finally, the primary radius is  $17 R_\odot$  [4], the binary separation is  $27.5 R_\odot$  [4], assuming  $\alpha = 0.8$  [5] we obtained a mass loss rate in the range  $(1.3 - 2.5) \times 10^{-6} M_\odot/\text{yr}$ . This result is on the upper fringe of values found for stars of the same luminosity of QV Nor from radio and UV data. On the other hand, it is consistent with the mass loss rate estimated by [3] using Ginga observations.

**Acknowledgements** Part of this work was supported by the Spanish *INTEGRAL: Observaciones multifrecuencia de sistemas binarios de rayos X* project number ESP2001-4541-PE and *International Gamma Ray Astrophysics Lab. Operaciones. C3* project number ESP2002-04124-C03-03. This research has made use of data obtained through the High Energy Astrophysics Science Archive Research Center Online Service, provided by the NASA/Goddard Space Flight Center.

## References

1. Abbott, D.C.: Radiatively driven stellar winds. *ApJ* **259**, 282–301 (1982)

2. Castor, J.I., Abbott, D.C., Klein, R.I.: Radiation-driven winds in Of stars. *ApJ* **422**, 157–174 (1975)
3. Clark, G.W., Woo, J.W., Nagase, F.: Properties of a B0 I stellar wind and interstellar grains derived from Ginga observations of the binary X-ray pulsar 4U 1538–52. *ApJ* **195**, 336–350 (1994)
4. Crampton, D., Hutchings, J.B., Cowley, A.P.: Optical spectroscopy and system parameters for 4U 1538–52. *ApJ* **259**, L63–L66 (1978).
5. Friend, D.B., Abbott, D.C.: The theory of radiatively driven stellar winds. III. Wind models with finite disk correction and rotation. *ApJ* **311**, 701–717 (1986).
6. Jahoda, K., Swank, J.H., Giles, A.B. et al.: In-orbit performance and calibration of the Rossi X-ray Timing Explorer (RXTE) Proportional Counter Array (PCA). *Proc. SPIE* (1996) doi: 10.1117/12.256034
7. Kreykenbohm, I., Coburn, W., Wilms, J. et al.: Confirmation of two cyclotron lines in Vela X–1. *A&A* **395**, 129–140 (2002)
8. Makishima, K., Koyama, K., Hayakawa, S., Nagase, F.: Spectra and pulse period of the binary X-ray pulsar 4U 1538–52. *ApJ* **314**, 619–628 (1987)
9. Makishima, K., Mihara, T., Nagase, F., Tanaka, Y.: Cyclotron resonance effects in two binary X-ray pulsars and the evolution of neutron star magnetic fields. *ApJ* **525**, 978–994 (1999)
10. Mihara, T.: Observational study of X-ray spectra of binary pulsars with Ginga. Ph.D. thesis, University of Tokyo (1995)
11. Rodes, J.J.: Análisis espectral en rayos X del sistema binario de alta masa 4U 1538–52/QV Nor. Ph.D. thesis, University of Alicante (2007)
12. Rodes, J.J., Torrejón, J.M., Bernabéu, G.: The fundamental cyclotron line in 4U 1538–52. In: Ulla, A., Manteiga, M. (eds.) *Lecture notes and essays in astrophysics III*. Stanford Linear Accelerator Center, Stanford (2008, in press)
13. Rotschild, R.E., Blanco, P.R., Gruber, D.E. et al.: In-flight performance of the high energy X-ray timing experiment on the Rossi X-ray Timing Explorer. *ApJ* **496**, 538–549 (1998)